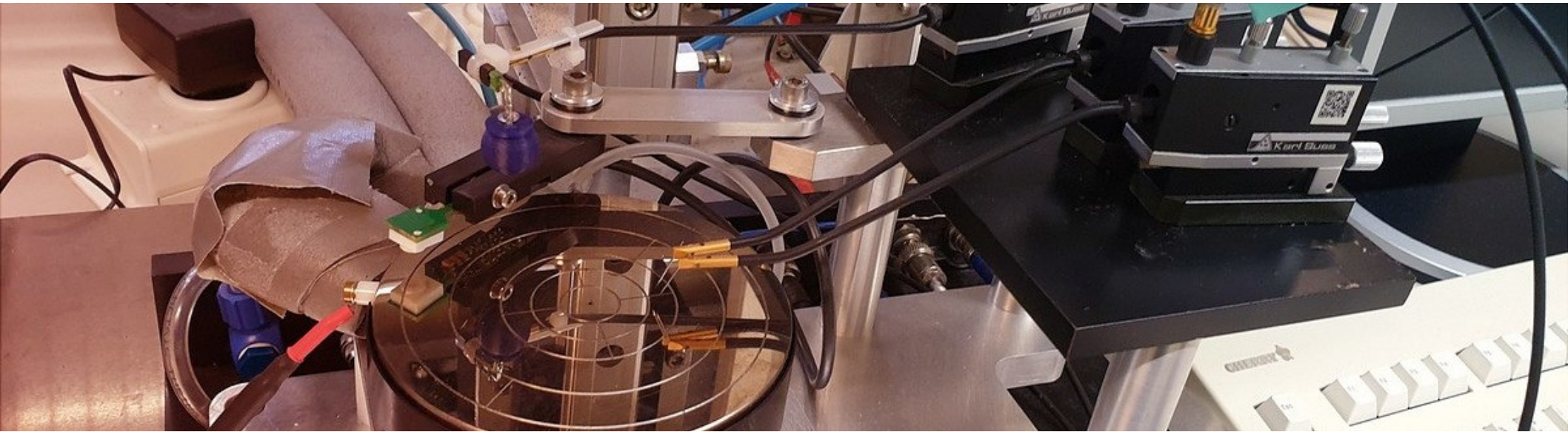


BiOi defects in LGADs



Chuan Liao^a, E. Fretwurst^a, E. Garutti^a, J.Schwandt^a, A.Vauth^a

^aInstitut für Experimentalphysik, Universität Hamburg

High-D Consortium

Feb 22, 2022



Universität Hamburg
DER FORSCHUNG | DER LEHRE | DER BILDUNG

I. Motivation

II. Displacement damage and B_iO_i defect

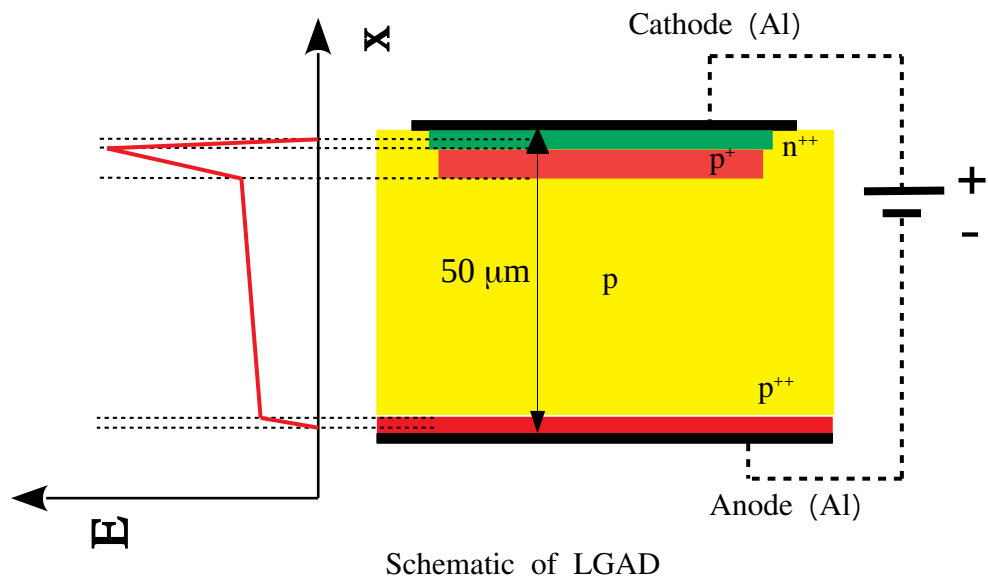
III. Experimental details

IV. Measurement results

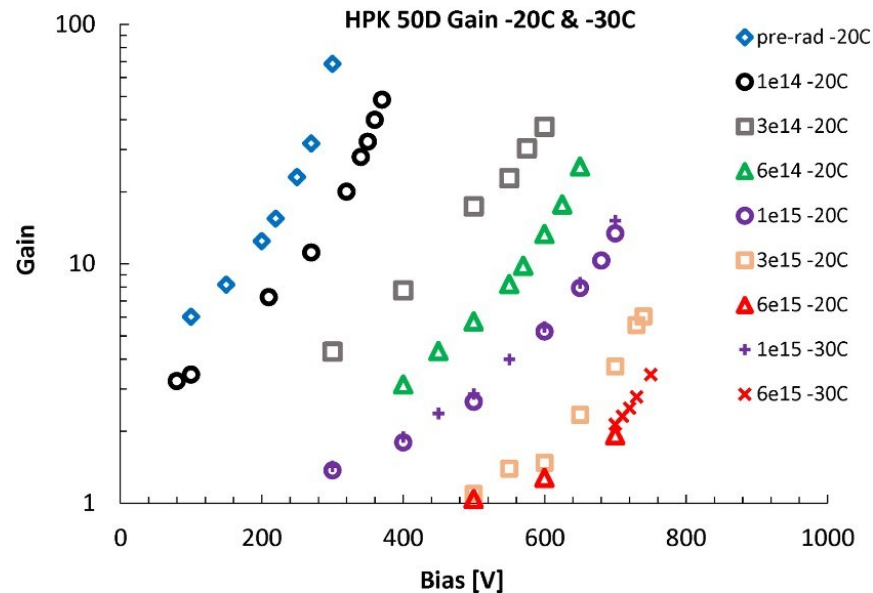
V. Summary

Motivation

Radiation damage of LGADs [1] (Low Gain Avalanche Diodes)



- Aluminum
- p type bulk (Boron doping, $\sim 10^{13} \text{ cm}^{-3}$)
- p⁺ (Boron doping B_s^- , $\sim 10^{16} \text{ cm}^{-3}$)
- p⁺⁺ (Boron doping B_s^- , $\sim 10^{19} \text{ cm}^{-3}$)
- n⁺⁺ (phosphorus doping P_s^+ , $\sim 10^{21} \text{ cm}^{-3}$)

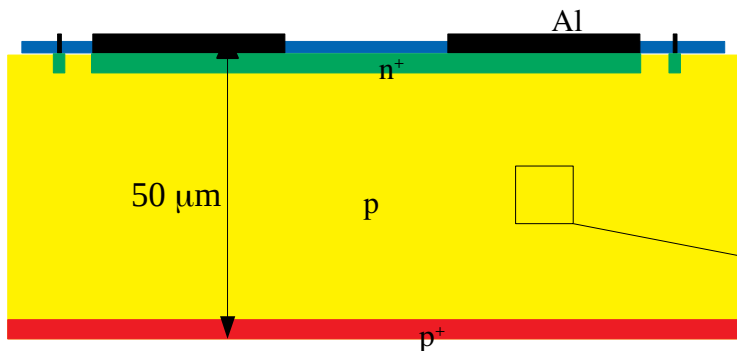


Gain value vs. bias for different fluences

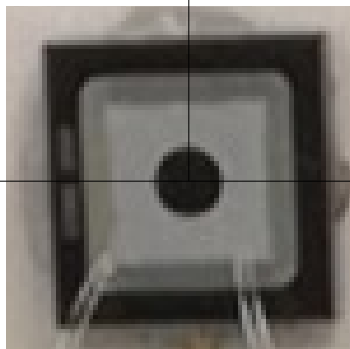
Significant decrease of Gain value after irradiation

[1] Kramberger, G., et al. "Radiation effects in Low Gain Avalanche Detectors after hadron irradiations." Journal of Instrumentation 10.07 (2015): P07006.

Motivation

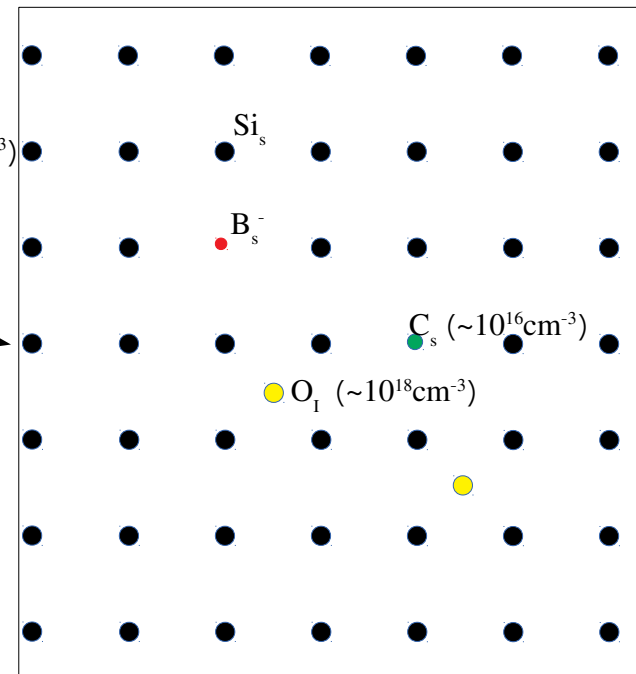
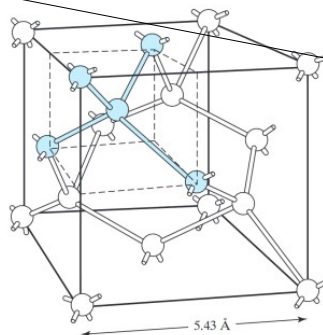


Cross section schematic of Silicon diodes (PIN diodes) we used



The top view of Silicon diodes (PIN diodes) we used

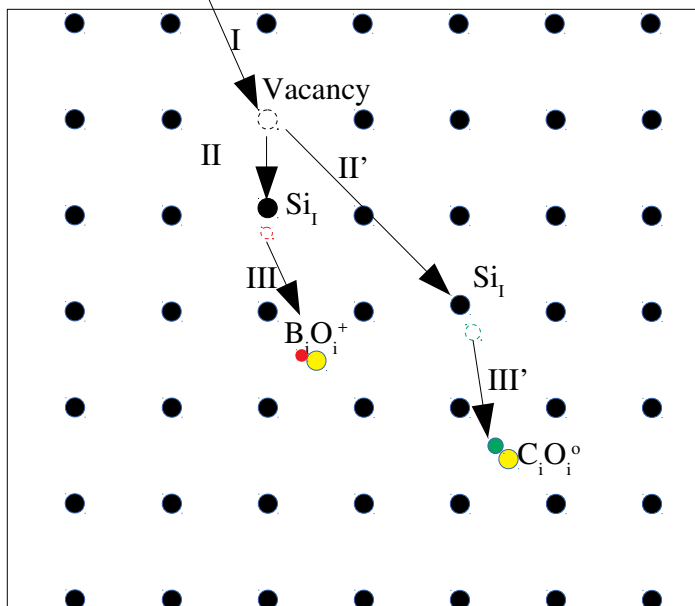
- Aluminum
- p type bulk (Boron doping, $10^{13} \sim 10^{15} \text{ cm}^{-3}$)
- p⁺ (Boron doping B_s^- , $\sim 5 \times 10^{19} \text{ cm}^{-3}$)
- n⁺ (phosphorus doping P_s^+ , $\sim 1 \times 10^{21} \text{ cm}^{-3}$)
- SiO₂



Schematic of Silicon crystal (cube side $a_0 = 5.431 \text{ \AA}$)
 N_{eff} (space charge density in the bulk, at room temperature)
 was determined by concentration of B_s^- or P_s^+ (p or n type)

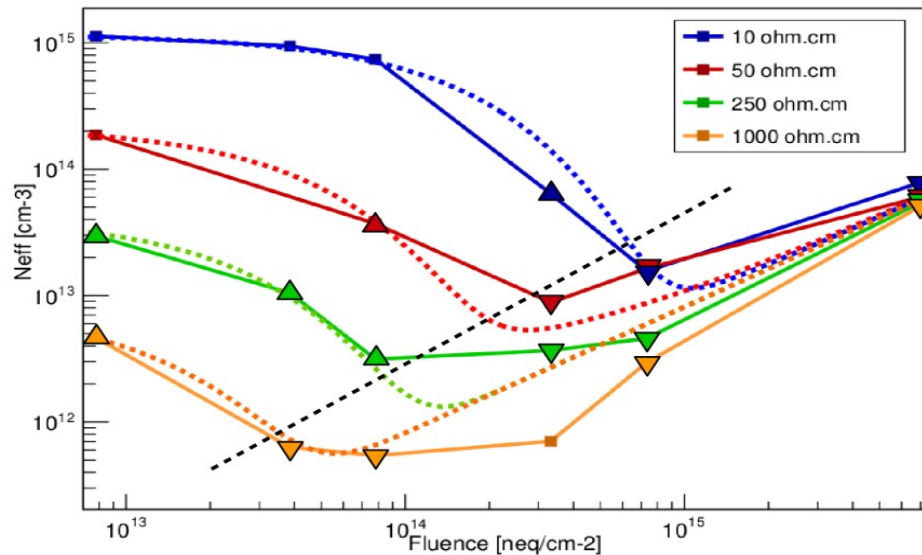
Radiation damage in p-type silicon sensor

High energy particle or Gamma-ray



Schematic of radiation damage in p-type silicon sensor

- I: Lattice Silicon atom (Si_s) was knocked out by incident particle and Si_s got recoil energy and turns to interstitial silicon (Si_i)
- II: Si_i diffusion in the bulk and impact on Lattice Boron atom (B_s)
- III: B_s was knocked out Si_i and turns to interstitial Boron (B_i) and finally captured by interstitial Oxygen (O_i)



N_{eff} vs. fluence for different initial doping concentration

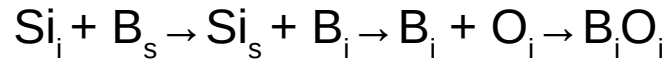
Radiation damage of p-type diodes is dominated by acceptor removal in the beginning and afterwards by acceptor generation [1]

B^- turn to B_iO_i^+

Change in N_{eff} is a factor of 2 and it will significantly affect the distribution of electric field.

Radiation damage in p-type silicon sensor


Microscopic behavior :



Macroscopic behavior

Increase of leakage current
Change of effective space charge density
Decrease of charge collection efficiency
Decrease of gain value in LGADs

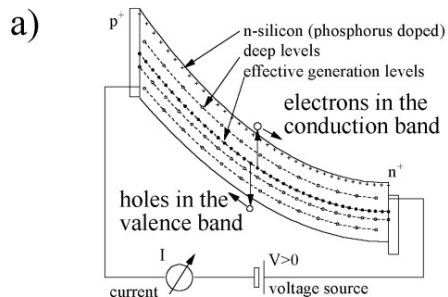
Many other defects like the shallow defects E(30K),
H(40K) and deep defects V_2 , V_3

- 
1. Impurity dependence (investigate PIN diodes with different resistivity)
 2. Irradiated particle dependence (investigate PIN diodes irradiated by different particles)
 3. Irradiation fluence dependence (investigate PIN diodes with different irradiation fluence)
 4. Annealing behavior (investigate PIN diodes after isothermal annealing at 80°C, and isochronal annealing from 100°C to 200°C)
 5. LGADs sensor (investigate LGADs sensor, such observed results compare to the results given by 1-4)

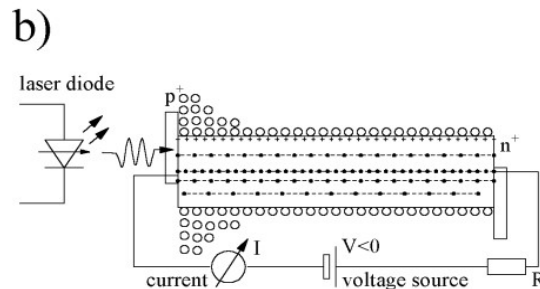
“The radiation damage induced defect in p-type silicon, BiOi is investigated”

Experimental principle

Basic Principle of Thermally Stimulated Current-TSC [2]:

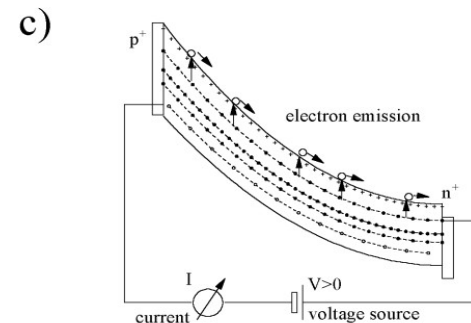


a) Cooling

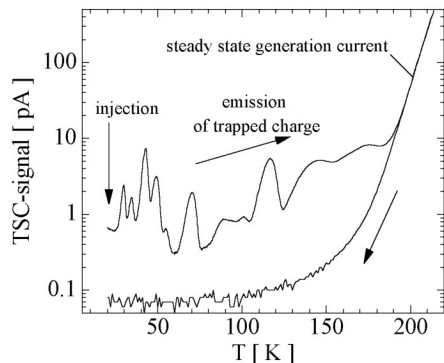


b) Injection:

Forward bias injection, light injection and majority carriers injection.



c) Recording data

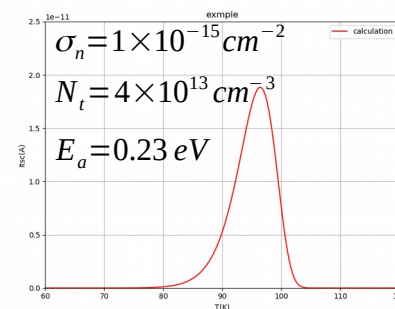


d). TSC spectrum [2]

$$I_{tsc} = \frac{1}{2} q_0 A d N_t e_n \exp\left(-\frac{1}{\beta} \int e_n(T) dT\right)$$

$$e_n = \sigma_n v_{th,n} N_c \times \exp\left(\frac{-E_a}{K_b T}\right)$$

$$E_a = E_C - E_T$$



e). example of calculated TSC peak

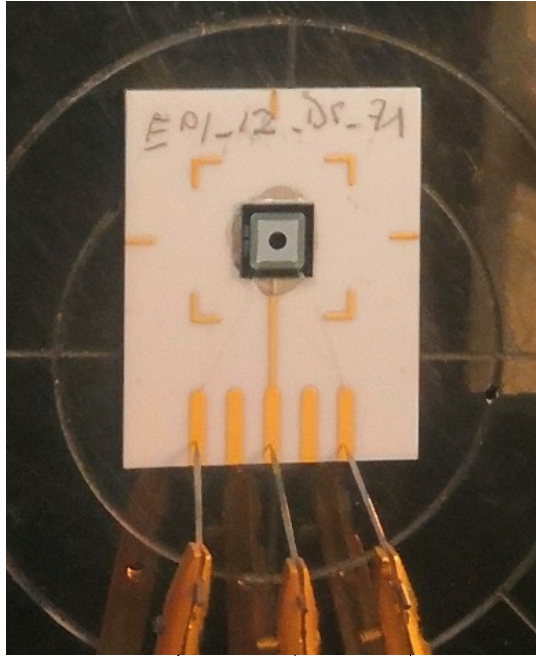
N_t is defect concentration; b is heating rate; s_n is capture cross section; E_a is activation energy; A is diodes area; d depleted thickness; [1]

[1] Buehler, M. G. Solid-State Electronics 15.1 (1972): 69-79.

[2] Moll, Michael. Radiation damage in silicon particle detectors: Microscopic defects and macroscopic properties. No. DESY-THESIS-1999-040. DESY, 1999.

Investigated diodes

Silicon pad detector

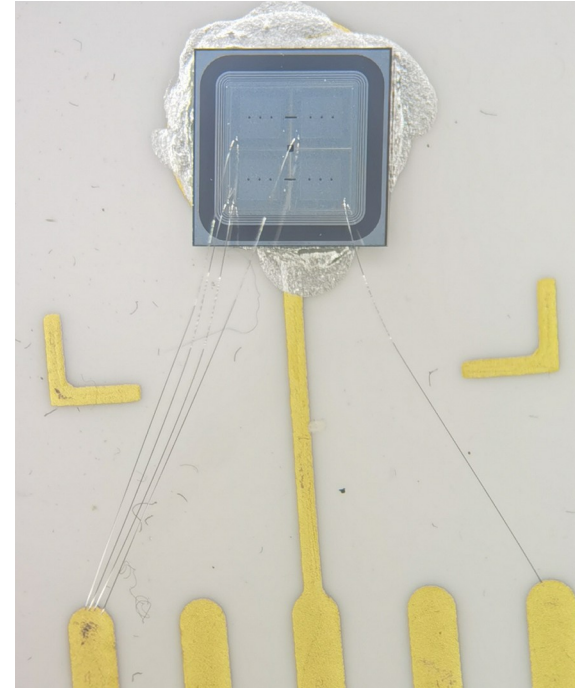


Guard ring

Pad

Back side:
bias voltage

LGADs
2x2 pixels

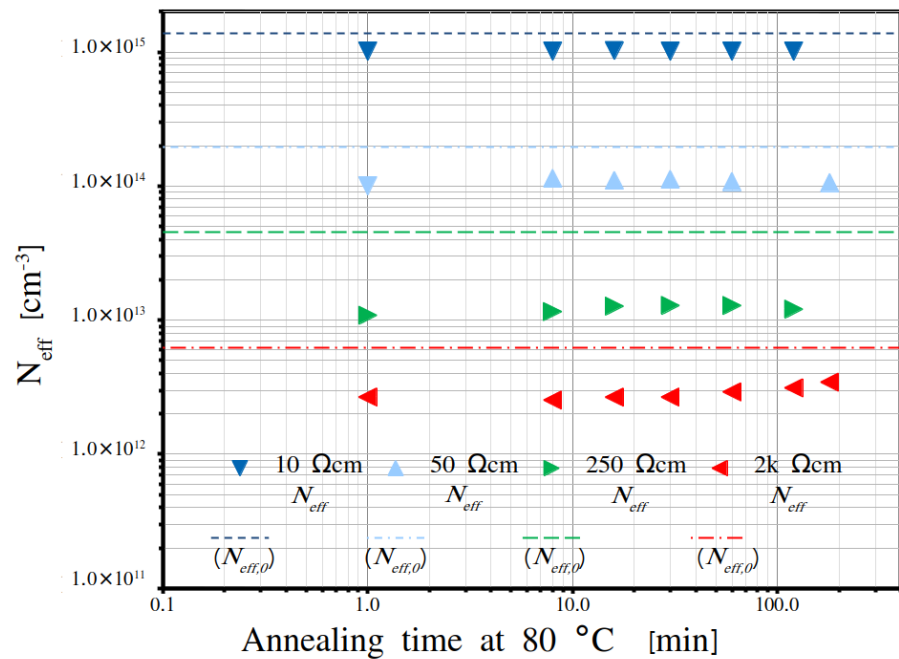


Guard ring
+3 pixels
grounded

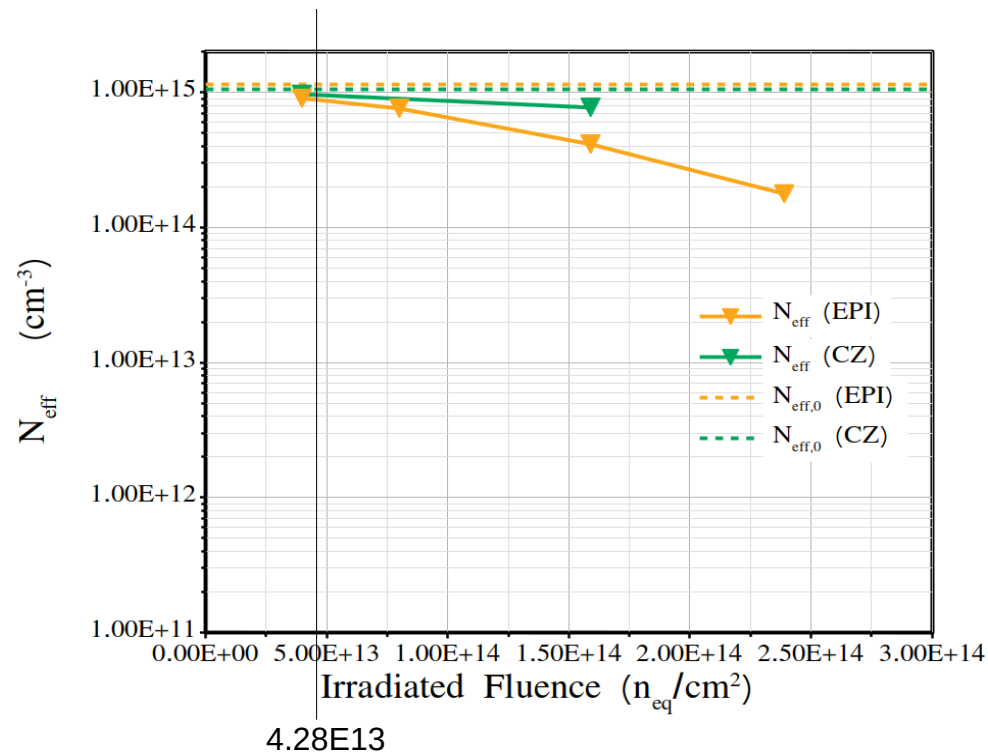
Back side:
bias voltage

Measured pixel

Effective doping

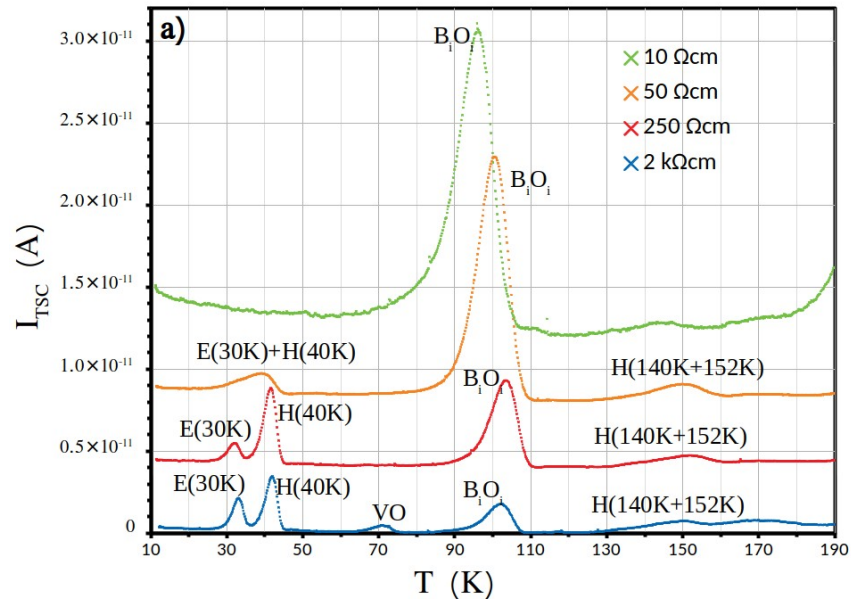


Effective doping for EPI diodes with different resistivity after irradiation by **23 GeV protons** with fluence value $4.28\text{E}13\ n_{eq}/\text{cm}^2$.

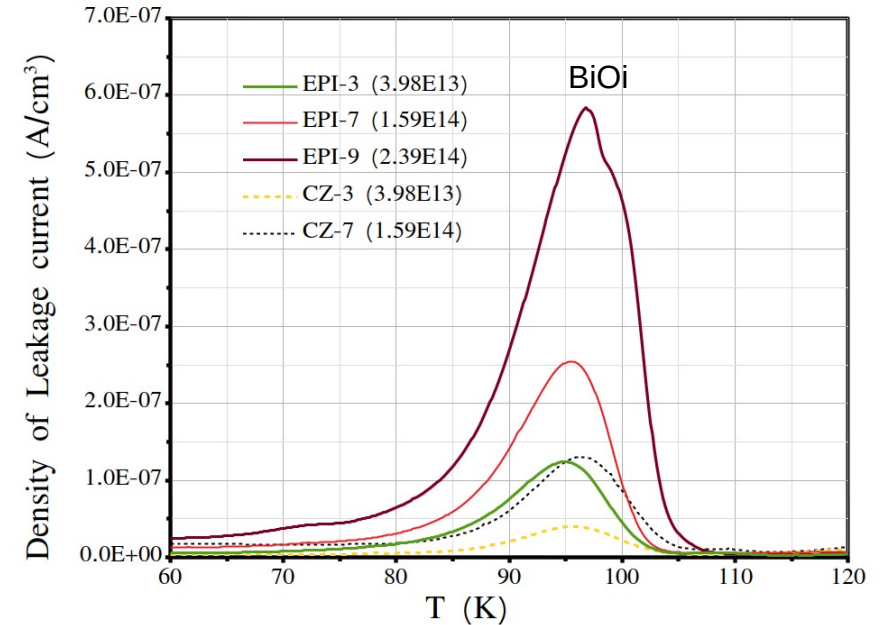


Effective doping for EPI- and CZ-diodes ($\sim 10\ \Omega\text{cm}$) after irradiation with **6 MeV electrons** with fluence values in the ranges between $3.98\text{E}13 \sim 2.39\text{E}14\ n_{eq}/\text{cm}^2$.

Thermally Stimulated Current

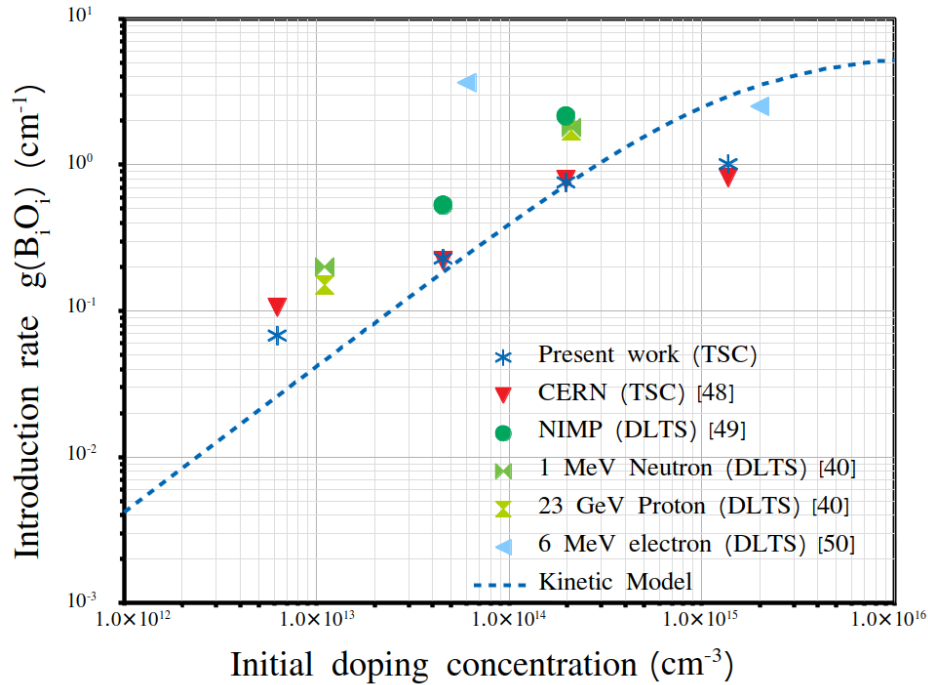


TSC spectra of diodes with different resistivity after **23 GeV protons** irradiation to $\Phi_{eq} = 4.28E13 \text{ n}_{eq}/\text{cm}^2$ for reverse bias 20 V (2 kΩcm), 40 V (250 Ωcm), 200 V (50 Ωcm) and 100 V (10 Ωcm, spectra normalized to $d/w(100 \text{ V})$).

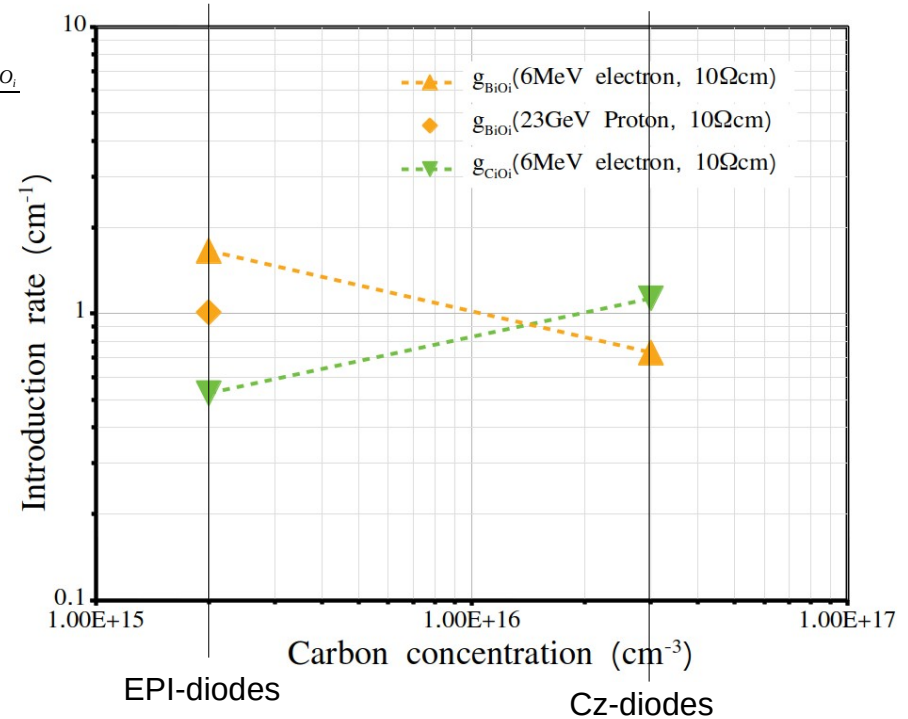


TSC spectra of diodes produced by **different processing** – Epitaxial (EPI-3, 7, 9) and Czochralski (CZ-3, 7) with 10 Ωcm resistivity, and after **6 MeV electrons** irradiation with fluence $\Phi = 1, 4, 6 \times 10^{15} \text{ cm}^{-2}$. The diodes were measured with applied reverse bias 100 V, and spectra are normalized by a factor $1/(Aw(T))$. A = active area, $w(T)$ = temperature dependent depletion depth at constant bias voltage

Introduction rate



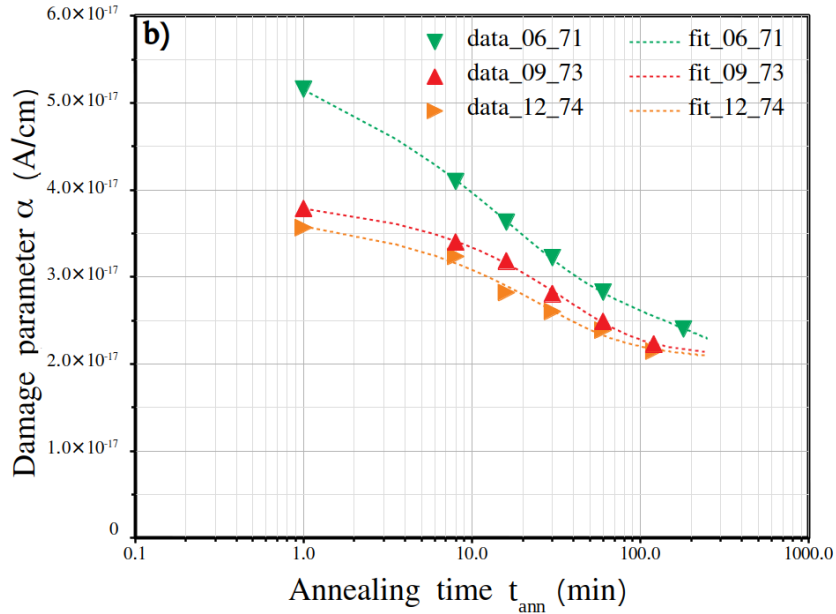
$$g(B_i O_i) = \frac{N_{t, B_i O_i}}{\phi_{eq}}$$



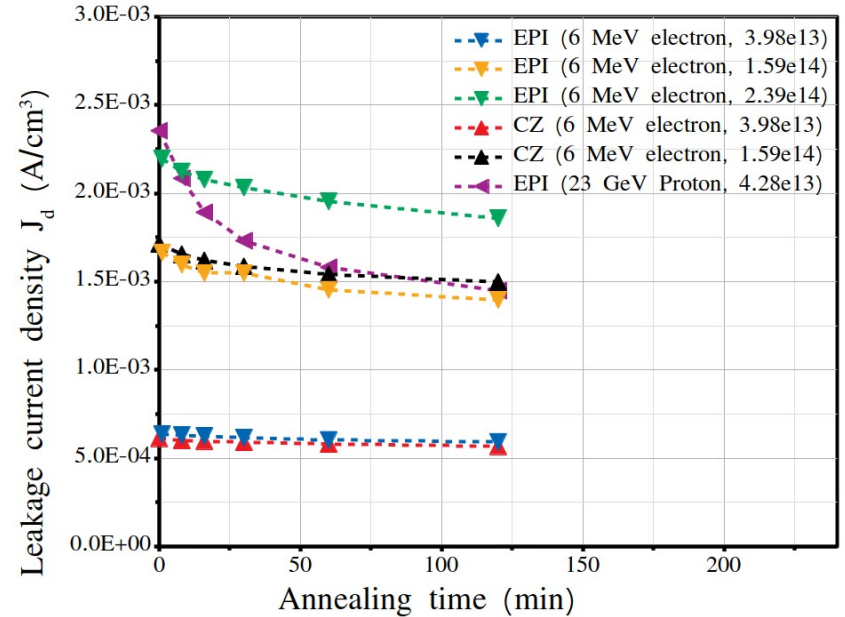
Introduction rate of $B_i O_i$ as function of initial doping ($\sim [B_s]$) for EPI-diodes

Introduction rate of $B_i O_i$ and $C_i O_i$ as function of Carbon concentration ($\sim [C_s]$)

Annealing behavior (80°C)

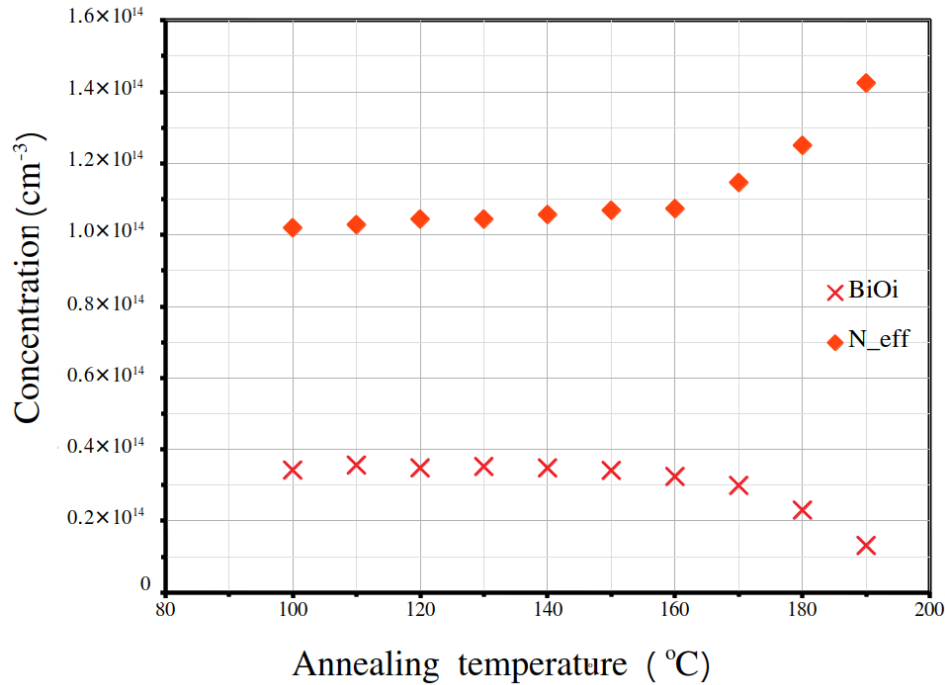


Annealing behavior of current related damage parameter for EPI- diodes with resistivity 2 k Ω cm (12_74), 250 Ω cm (09_73) and 50 Ω cm (06_71), which were irradiated by 23 GeV protons with fluence $\Phi_{\text{eq}} = 4.28\text{E}13 \text{ cm}^{-2}$

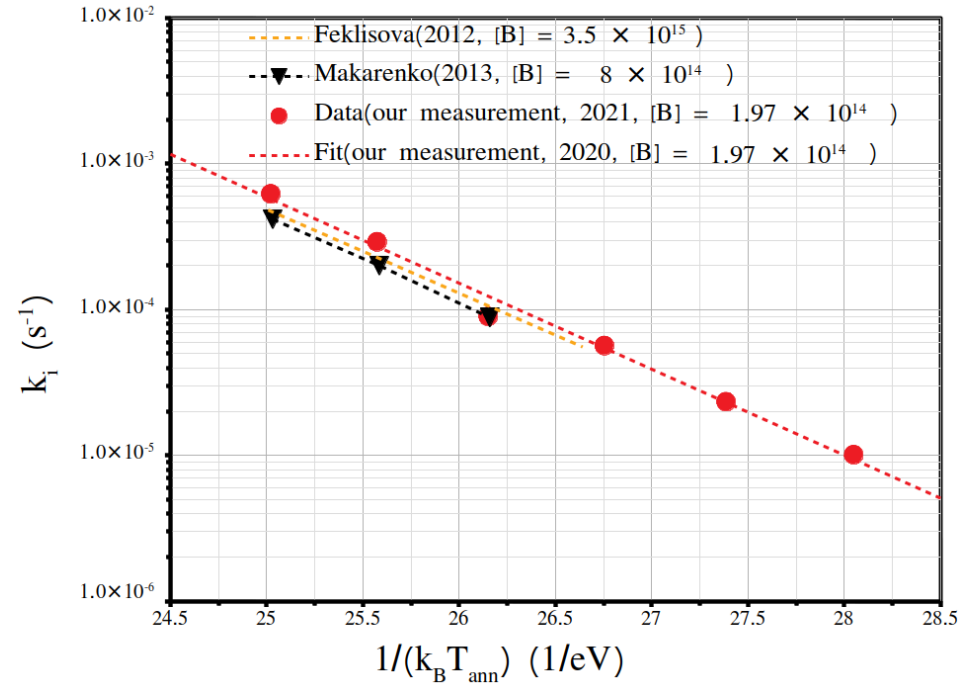


Annealing behavior of leakage current for EPI- and Cz- diodes with resistivity 10 Ω cm, and irradiated by different particles and fluence values

Isochronal annealing behavior of B_iO_i



Defect concentration [B_iO_i] and N_{eff} vs. annealing temperature. For each temperature step the duration of annealing was 15 min



The frequency factors for annealing out of B_iO_i vs. $1/(k_B T_{ann})$; from the slope the corresponding activation energy of B_iO_i is extracted to $E_A = 1.35 \pm 0.01$ eV

Summary

I. Impurity dependence:

- Higher initial doping concentration leads to higher B_iO_i introduction rate after the same fluence value, but the increase is limited
- The diodes with high carbon concentration restrain the generation of B_iO_i and, thus, depress the deactivation of $[B_s]$

II. Fluence dependence:

- The higher irradiation fluence value leads to higher B_iO_i concentration (up to now)
- The higher irradiation fluence value leads to higher leakage current, and the annealing out of ΔI increasing with irradiation fluence value

III. Particle dependence:

- The generation of B_iO_i for 23 GeV proton approx equal to half of value for 6 MeV electron
- The larger annealing out value of ΔI was observed on 23 GeV proton irradiated diodes compare to 6 MeV electron irradiated

IV. Annealing behaviors:

- If $T_{\text{ann}} > 150 \text{ }^\circ\text{C}$, $[B_iO_i]$ decrease, N_{eff} increase
- The change $\Delta N_{\text{eff}} \approx 2 \times \Delta N_t ([B_iO_i])$ as expected from $B_s(-) \rightarrow B_iO_i(+)$

V. LGAD diodes:

- The measurements of the pixel sensors with and without wire-bond were performed in our lab
- Up to now the analysis of the data was not as we expected

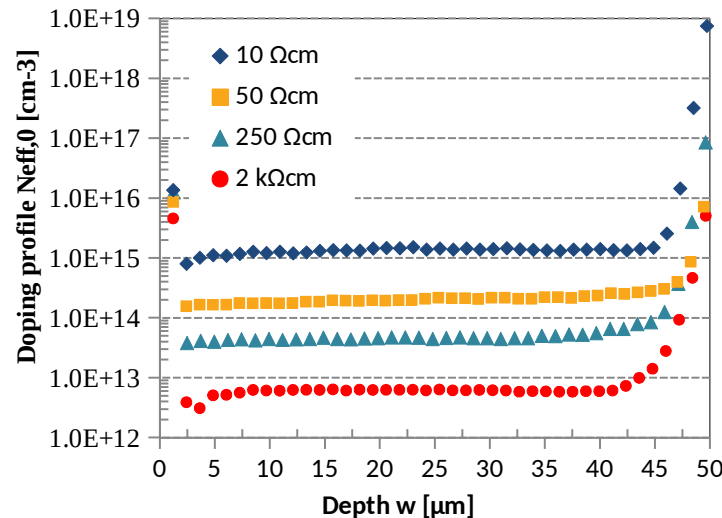
Back Up

Experimental details

Experimental detail

Information of measured epitaxial silicon diodes (PIN)

Label	EPI50P_01_DS_73	EPI50P_06_DS_71	EPI50P_09_DS_73	EPI50P_12_DS_74
$N_{\text{eff},0}$	$1.37\text{E}15 \text{ cm}^{-3}$	$1.97\text{E}14 \text{ cm}^{-3}$	$4.53\text{E}13 \text{ cm}^{-3}$	$6.24\text{E}12 \text{ cm}^{-3}$
Irradiation	23 GeV proton, $\Phi = 6.91\text{E}13 \text{ cm}^{-2}$, neutron equivalence $\Phi_{\text{eq}} = 4.28\text{E}13 \text{ cm}^{-2}$			
Area	$6.927\text{E}-2 \text{ cm}^2$			
Thickness	50 μm			



$N_{\text{eff},0}$ vs. Depth from ITME(Institute of Electronic Materials Technology)

Experimental detail

Information of measured silicon diodes

Label	EPI50P_06_DS_3	EPI50P_06_DS_7	EPI50P_06_DS_9	CZ300P_06_DS_3	CZ300P_06_DS_7
$N_{\text{eff},0}$	Expitaxial silicon, P-type $1.15 \times 10^{15} \text{ cm}^{-3}$			Cz silicon, P-type $1.05 \times 10^{15} \text{ cm}^{-3}$	
Initial resistivity	$\sim 10 \text{ } \Omega\text{cm}$			$\sim 10 \text{ } \Omega\text{cm}$	
Irradiation (6 MeV electrons)	$1 \times 10^{15} \text{ e/cm}^2$ ($3.98 \times 10^{13} n_{\text{eq}}/\text{cm}^2$)	$4 \times 10^{15} \text{ e/cm}^2$ ($1.59 \times 10^{14} n_{\text{eq}}/\text{cm}^2$)	$6 \times 10^{15} \text{ e/cm}^2$ ($2.39 \times 10^{14} n_{\text{eq}}/\text{cm}^2$)	$1 \times 10^{15} \text{ e/cm}^2$ ($3.98 \times 10^{13} n_{\text{eq}}/\text{cm}^2$)	$4 \times 10^{15} \text{ e/cm}^2$ ($1.59 \times 10^{14} n_{\text{eq}}/\text{cm}^2$)
Area	$6.21 \times 10^{-2} \text{ cm}^2$			$2.9 \times 10^{-2} \text{ cm}^2$	
Thickness	$50 \text{ } \mu\text{m}$			$350 \text{ } \mu\text{m}$	

C-V, I-V:



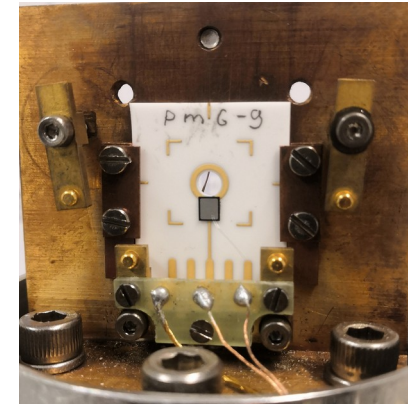
Experimental parameter (C-V, I-V):

Temperature: $20 \text{ } ^\circ\text{C}$
 Humidity: $< 10\%$
 Frequencies for C-V: 230 Hz, 455 Hz, 1 kHz, 10 kHz
 AC voltage for C-V: 0.5 V

Experimental parameter (TSC and TS-Cap):

Cooling down bias: 0 V
 Filling temperature: typical 10 K
 Filling: Forward bias filling, 0 V filling or light injection
 Filling time: 30 s
 Delay time: 30 s
 Heating rate: 0.183 K/s

Thermally stimulated current and Thermally stimulated capacitance (TSC, TS-Cap):



Experimental detail

Thermally Stimulated Current-TSC:

LED support for
light injection

Temperature
controller

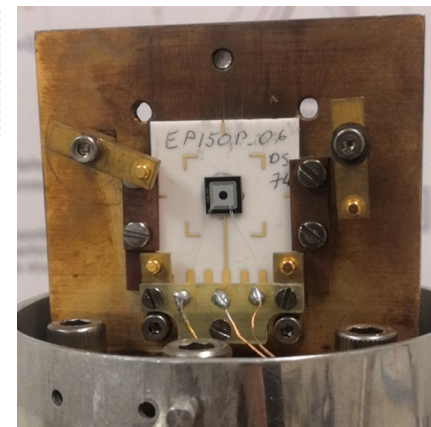
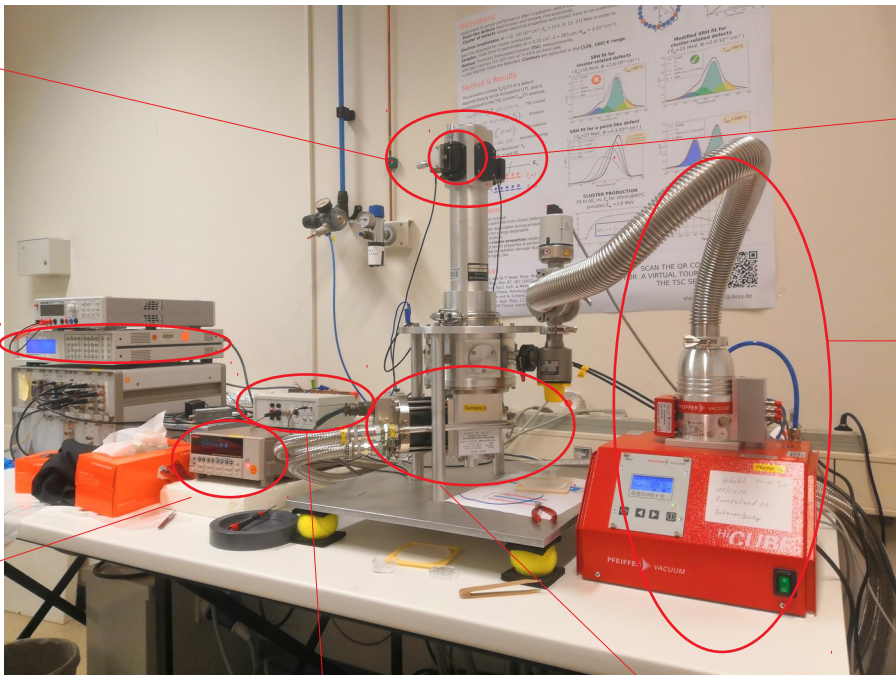
Keithly
6517A
Electrometer

Switch box for PC control of He
compressor and power supply for light
injection

Cooling system

Hot stage with sample
holder, temperature
sensor and heater

High vacuum
pump system



Experimental parameter (TSC):

Cooling down bias: 0 V
Filling temperature: typical 10 K
Filling: Forward bias filling, 0 V filling or light
injection
Filling time: 30 s
Delay time: 30 s
Heating rate: 0.183 K/s
Heating up bias: depends on effective space
charge concentration after irradiation

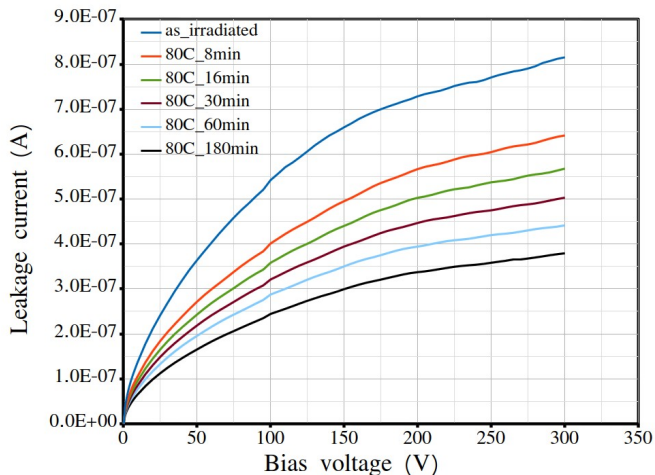
Methods for I-V and C-V measurements



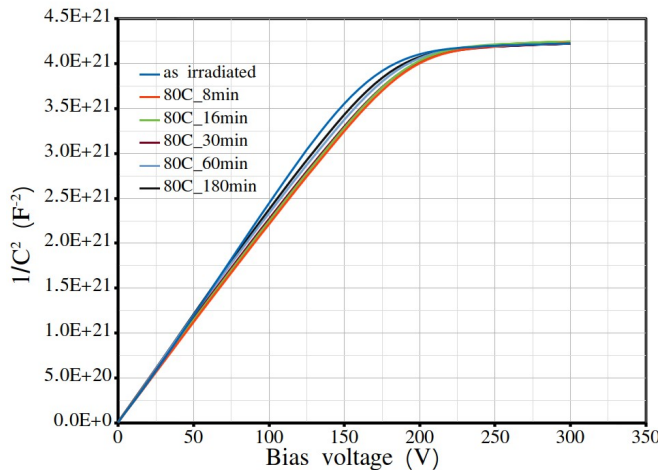
Universität Hamburg

DER FORSCHUNG | DER LEHRE | DER BILDUNG

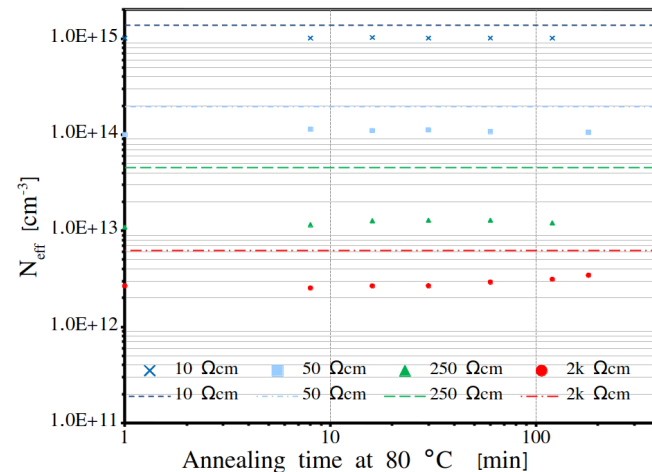
C-V, I-V measurement – isothermal annealing



I-V for $N_{\text{eff},0} = 1.97\text{E}14 \text{ cm}^{-3}$ diodes



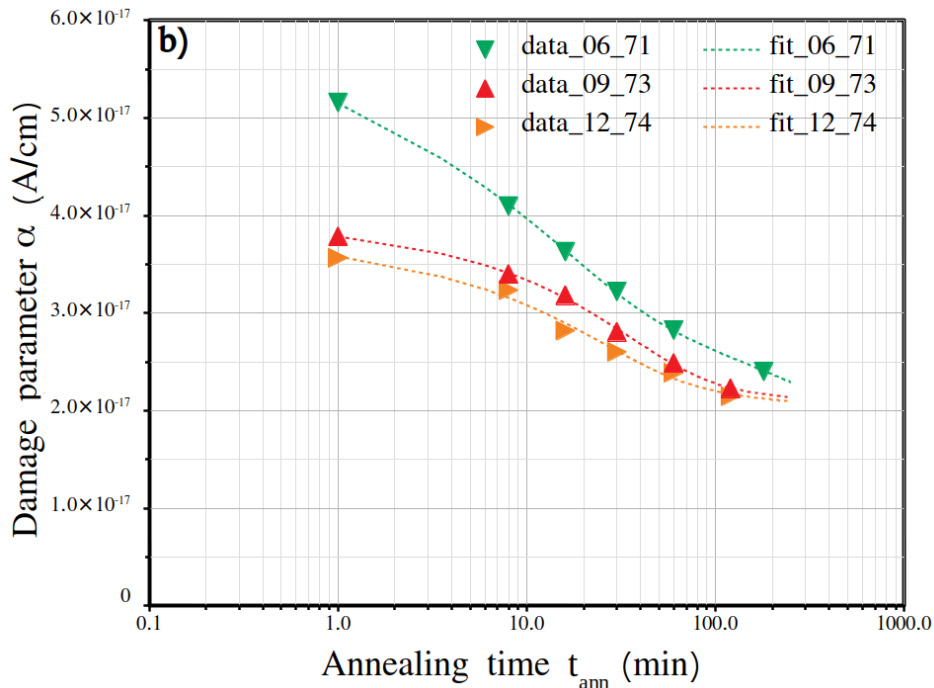
C-V for $N_{\text{eff},0} = 1.97\text{E}14 \text{ cm}^{-3}$ diodes



N_{eff} vs t_{ann} for $N_{\text{eff},0} = 1.97\text{E}14 \text{ cm}^{-3}$ diodes

- I. The decreases of leakage current after isothermal annealing
- II. Stability of effective doping concentration N_{eff} (full depleted voltage V_{fd}) during isothermal annealing

Annealing of current and full depletion voltage



$$\alpha = \frac{I}{V \phi_{eq}}$$

Fitting functions[1]: $\alpha(t) = \alpha_I \cdot \exp\left(\frac{-t}{\tau_I}\right) + \alpha_0 - \beta \cdot \ln\left(\frac{t}{t_0}\right)$ $t_0 = 1 \text{ min}$
 Fit parameter(50 Ωcm):

$$\alpha_I \approx 1.14 \times 10^{-17} \text{ A/cm}$$

$$\tau_I \approx 18 \text{ min}$$

$$\alpha_0 \approx 5.48 \times 10^{-17} \text{ A/cm}$$

$$\beta_0 \approx 4.51 \times 10^{-18} \text{ A/cm}$$

Ref. [1]:

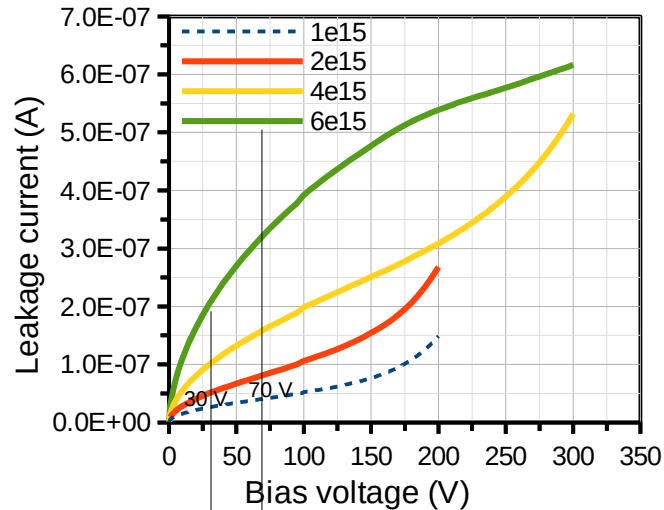
$$\alpha_I \approx 1.13 \times 10^{-17} \text{ A/cm}$$

$$\tau_I \approx 9 \text{ min}$$

$$\alpha_0 \approx 4.23 \times 10^{-17} \text{ A/cm}$$

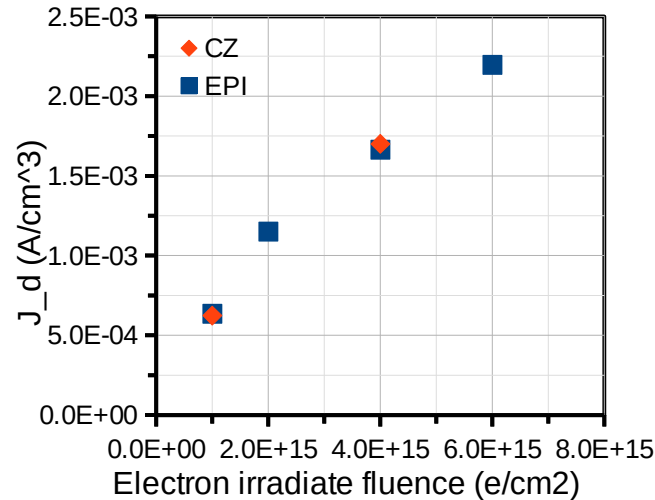
$$\beta_0 \approx 2.83 \times 10^{-18} \text{ A/cm}$$

I-V and N_{eff} profile (10 Ωcm , as-irrad)

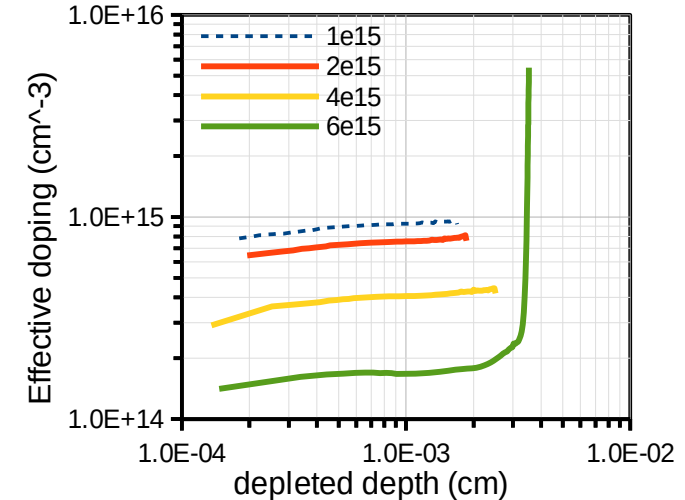


Averaged ranges to get density of leakage current (30V ~ 70V)

Leakage current for different fluence



Mean value of leakage current density J_d as function of irradiation fluence



Doping profile

- Leakage current increases with fluence. In order to observe the mean value of leakage current density (J_d), the current in the range from 30V to 70V was chosen for calculate J_d (the depleted volume is taken from C-V measurement)
- Doping profile is taken from C-V measurement with frequency equal 10 kHz and $V_{\text{AC}}=0.5\text{V}$. Effective doping decrease with fluence

TSC Data analyze

BiO_i in TSC spectra (1.97E14 cm⁻³)

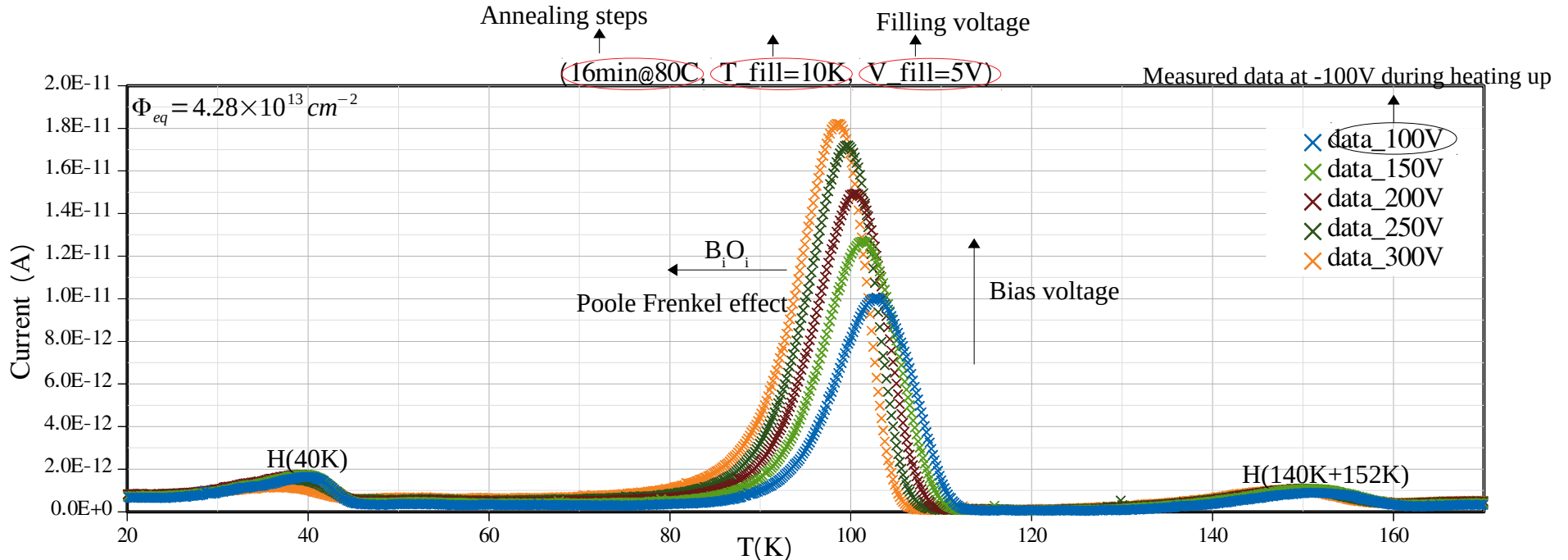
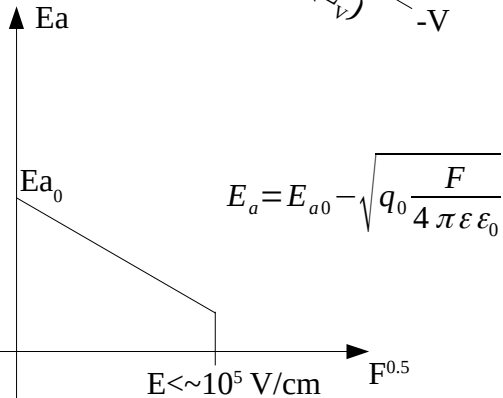
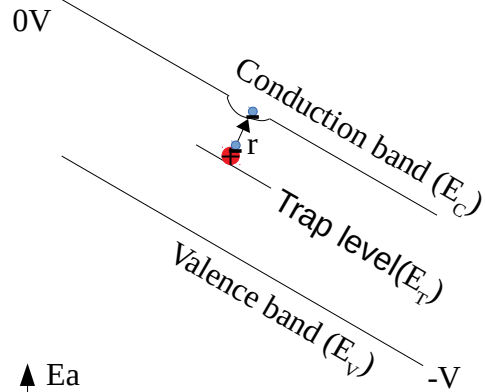


Fig 6. TSC spectra for different bias voltages of 50 Ωcm diode after 23 GeV proton irradiation

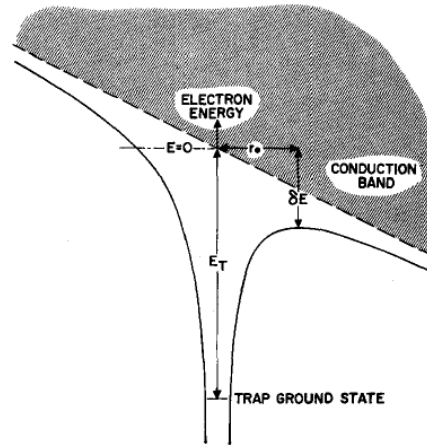
- Dominant BiO_i signal
- Shift of peak maximum with V_{bias} → Poole-Frenkel effect; electron trap BiO_i (o/+) donor defect
- Peak amplitude increases with bias voltage due to increasing depletion depth and after full depletion extending into the p+ region

Poole Frenkel effect

Example for 1-D[1]:



3-D [2]:



$$E_a = E_{a0} - \sqrt{\frac{q_0 F \cos \theta}{4\pi\epsilon\epsilon_0}}$$

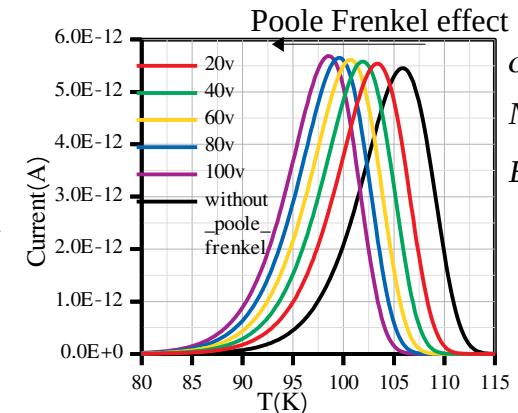
$$e_n = \sigma_n v_{th,n} N_c \times \exp\left(\frac{-E_{a0}}{k_B T}\right) \left[\left(\frac{1}{\gamma^2}\right) (e^\gamma (\gamma - 1) + 1) + \frac{1}{2} \right]$$

$$\gamma = (qF/\pi\epsilon_0\epsilon_r)^{1/2} q_0 / (k_B T)$$

Describe TSC peak:

$$I_{isc} = \frac{1}{2} q_0 A d N_t e_n(\sigma_n, E_a, T) \exp\left(-\frac{1}{\beta} \int e_n(\sigma_n, E_a, T) dT\right)$$

q_0 : elementary charge; A : area; d : depleted thickness; N_t : defect concentration; e_n : emission rate; T : temperature; x : position; β : heating rate; σ_n : electron captured cross section; $v_{th,n}$: thermal velocity of electron; N_c density of state in the conduction band; E_{a0} : zero field activation energy; k_B : Boltzmann constant; $F(x)$: electric field.



$$\sigma_n = 1 \times 10^{-15} \text{ cm}^{-2}$$

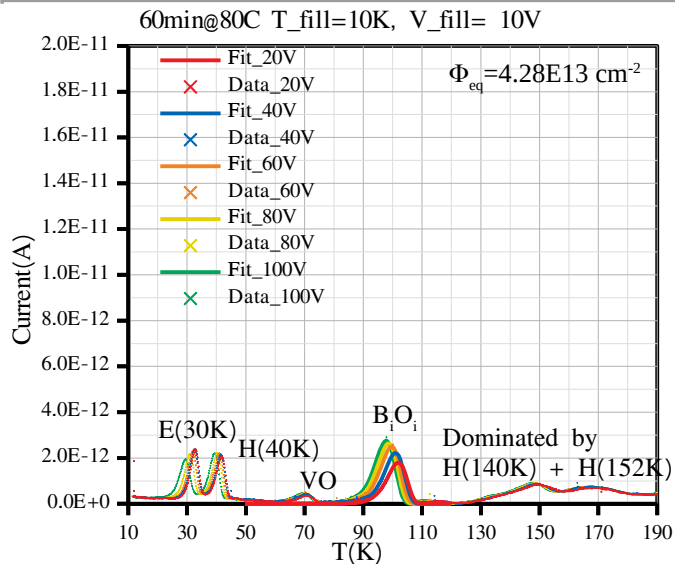
$$N_t = 1.2 \times 10^{13} \text{ cm}^{-3}$$

$$E_{a0} = 0.255 \text{ eV}$$

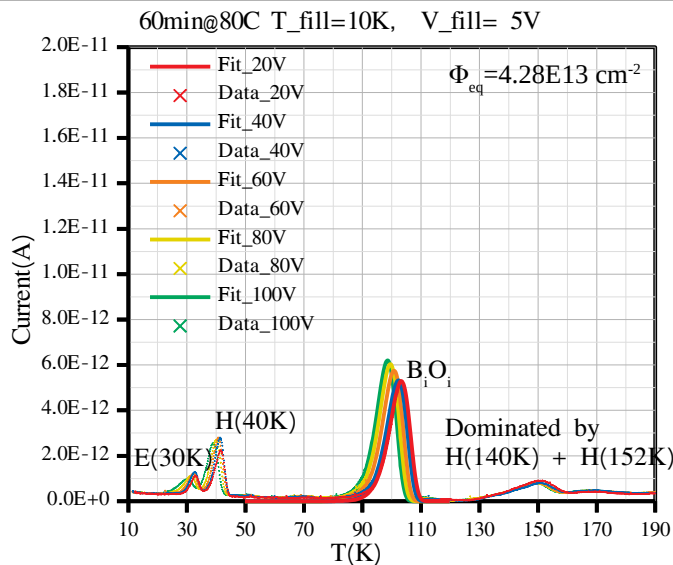
[1] J. L. Hartke, J. Appl. Phys. 39, 4871 (1968).

[2] Pintilie, I., E. Fretwurst, and G. Lindström. Applied Physics Letters 92.2 (2008): 024101.

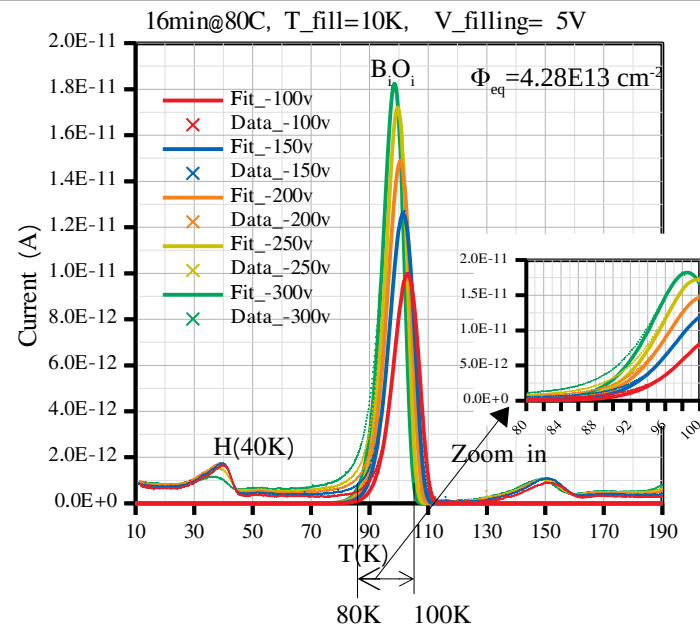
Fit B_iO_i peak in TSC spectra



TSC spectra for $N_{\text{eff},0} = 6.94E12 \text{ cm}^{-3}$ diodes with different V_{bias}



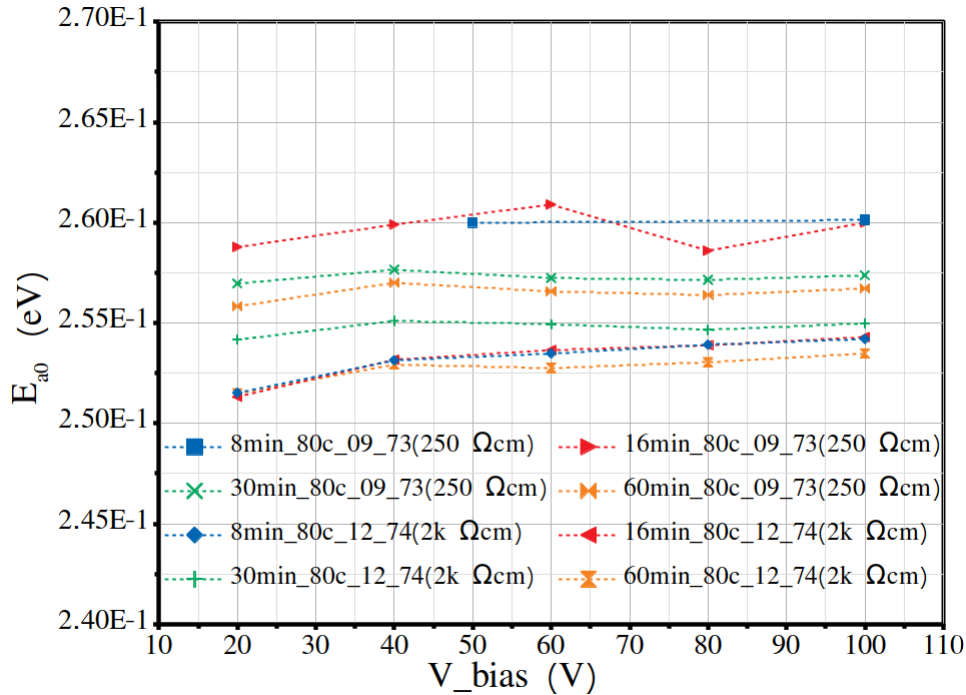
TSC spectra for $N_{\text{eff},0} = 4.53E13 \text{ cm}^{-3}$ diodes with different V_{bias}



TSC spectra for $N_{\text{eff},0} = 1.97E14 \text{ cm}^{-3}$ diodes with different V_{bias}

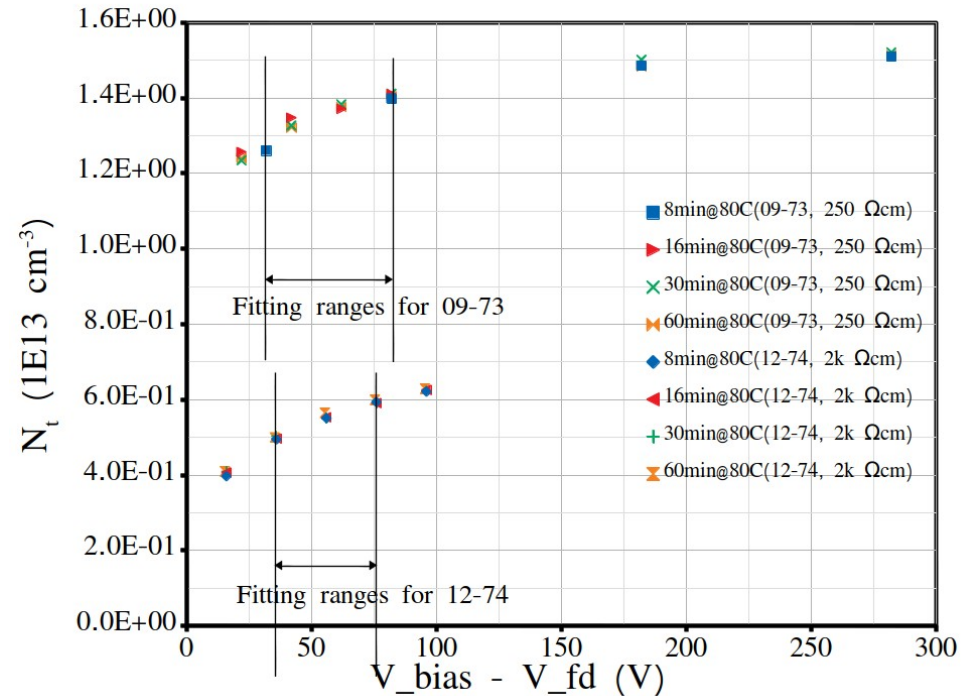
For same irradiation fluence, the B_iO_i concentration increase as $N_{\text{eff},0}$ increasing. And if most of the recoil energy deposited forms B_iO_i defect, the concentration of other defects will decrease

Activation energy and defect concentration



Zero field activation energy E_{a0} versus bias voltage of BiOi defect extracted from TSC spectra of 250 Ω cm and 2K Ω cm

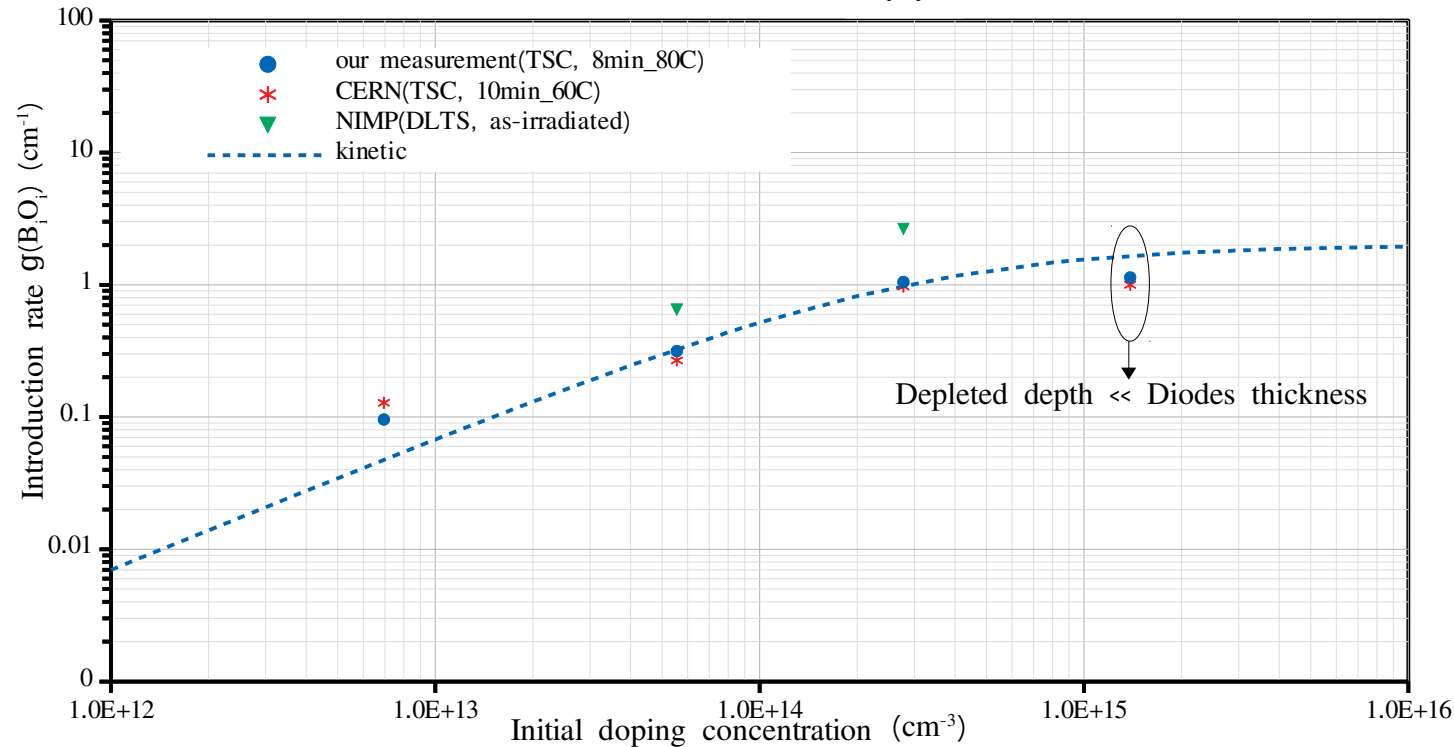
$$\sigma_n \approx 1 \times 10^{-15} \text{ cm}^{-2}$$



BiO_i concentration as function of excess voltage ($V_{bias} - V_{fd}$) for the 250 Ω cm and 2k Ω cm extracted from TSC spectra measured after annealing steps between 8 min and 60 min at 80°C. The ranges for a linear fit to the data are indicated for both diodes in order to get the BiO_i concentration at $V_{bias} = V_{fd}$

Introduction rate of B_iO_i for different doping

Introduction rate of B_iO_i



Definition of $g(B_iO_i)$:

$$g(B_iO_i) = \frac{N_{t,B_iO_i}}{\phi_{eq}}$$

Defect Kinetics Model [1-2]:

$$g(B_iO_i) \approx g_I \times \left(1 + \frac{k_{IC}[C_s]}{k_{IB}[B_s]}\right)^{-1}$$

$$g_I \approx 2 \text{ cm}^{-1}$$

$$\frac{k_{IB}}{k_{IC}} \approx 7$$

$$[C_s] \approx 2 \times 10^{15} \text{ cm}^{-3}$$

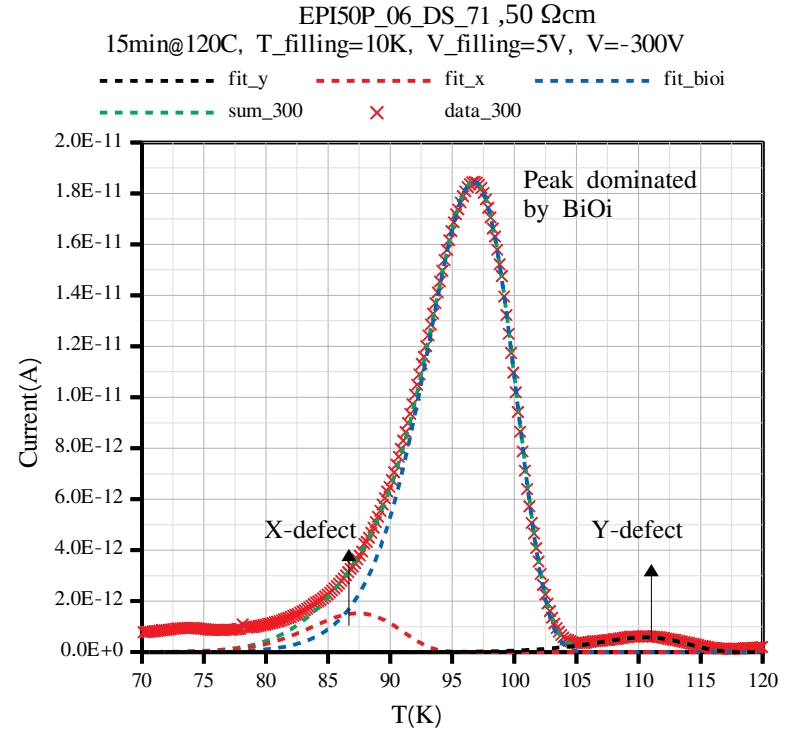
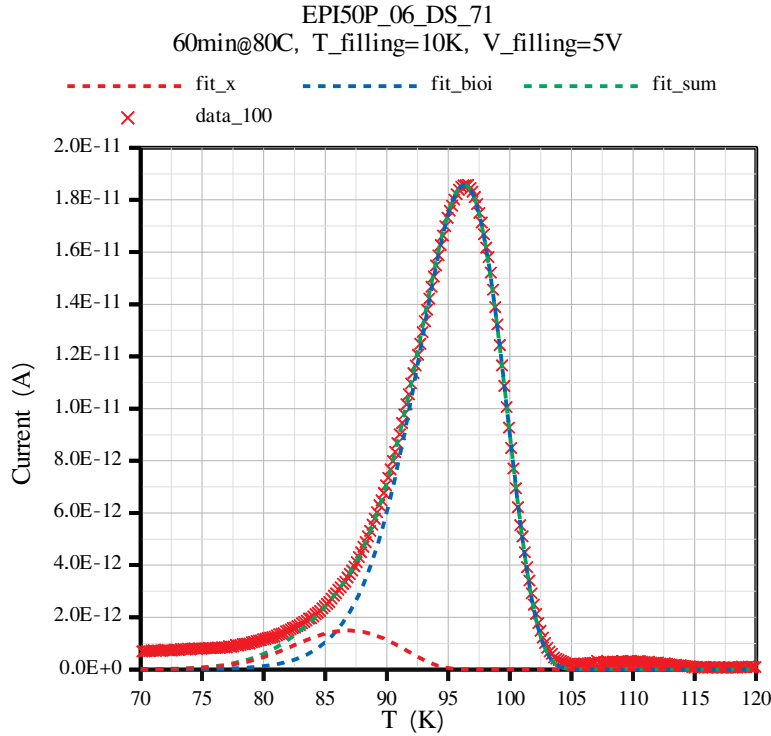
For higher initial doping ($N_{\text{eff},0} > 1\text{E}15 \text{ cm}^{-3}$), There appears to be some limit for the increase of $g(B_iO_i)$ --> for higher $N_{\text{eff},0} > 1\text{E}15 \text{ cm}^{-3}$,

If $N_{\text{eff},0}$ improved, the radiation hardness improves as well

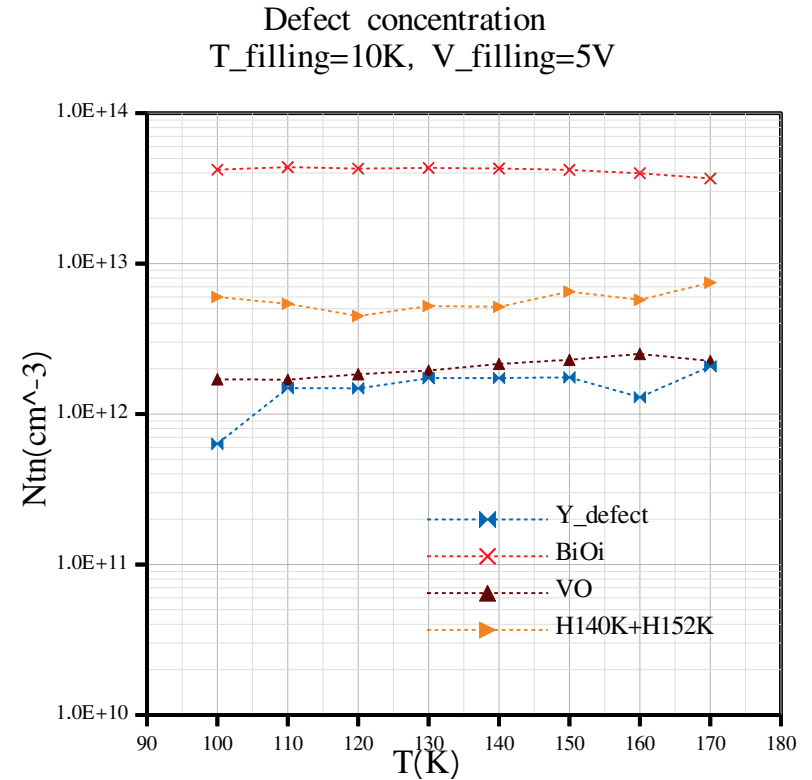
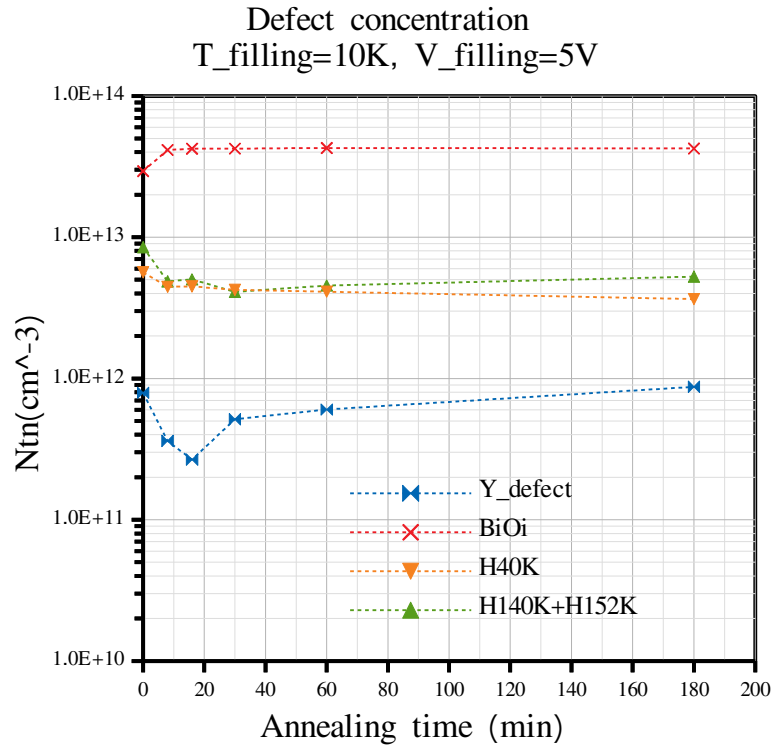
[1] Makarenko, Leonid F., et al. physica status solidi (a) 216.17 (2019): 1900354.

[2] Moll, Michael. "Acceptor removal-Displacement damage effects involving the shallow acceptor doping of p-type silicon devices." (2019).

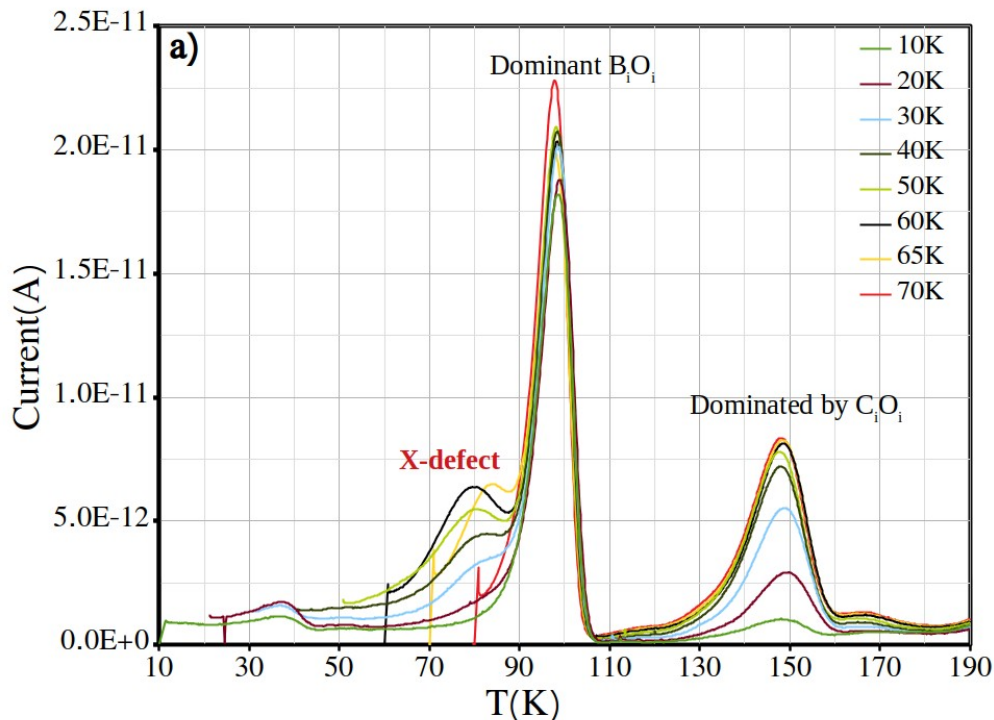
Annealing behavior of TSC measurements



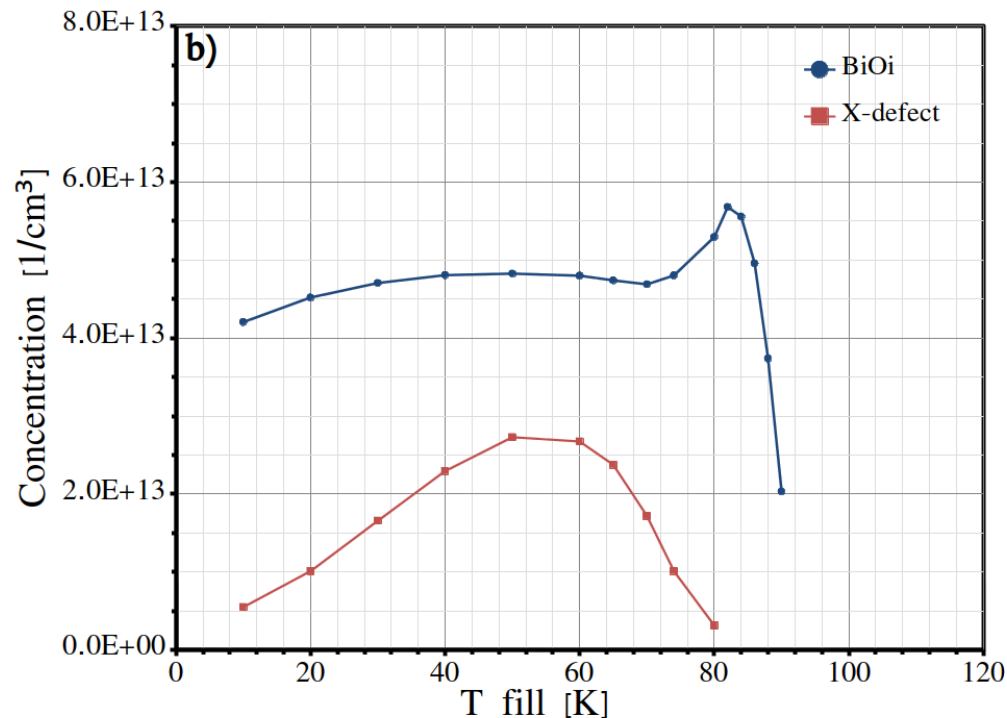
Annealing behavior of TSC measurements



Indication for X-defect ($1.97\text{E}14 \text{ cm}^{-3}$)



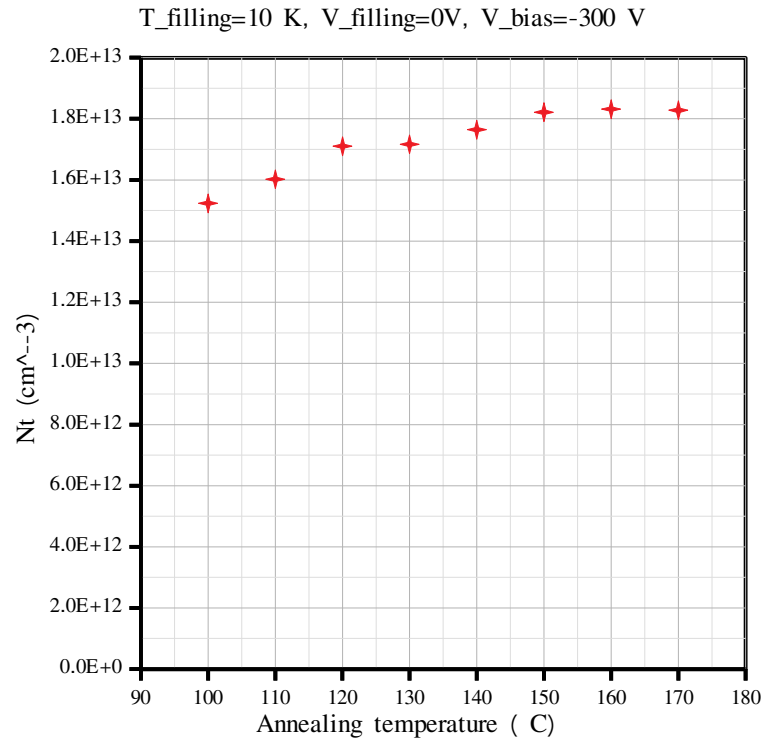
TSC spectrum of $N_{\text{eff},0} = 1.97\text{E}14 \text{ cm}^{-3}$ p-type diodes after 30 minutes isothermal annealing at 80°C . Different T_{fill} from 10K to 70K, $V_{\text{fill}} = 5\text{V}$



Concentration of BiO_i and X-defect versus filling temperature T_{fill} extracted from the TSC spectra

Forward bias injection:
$$p_t = \frac{N_t}{\left(1 + \frac{c_n}{c_p}\right)}$$

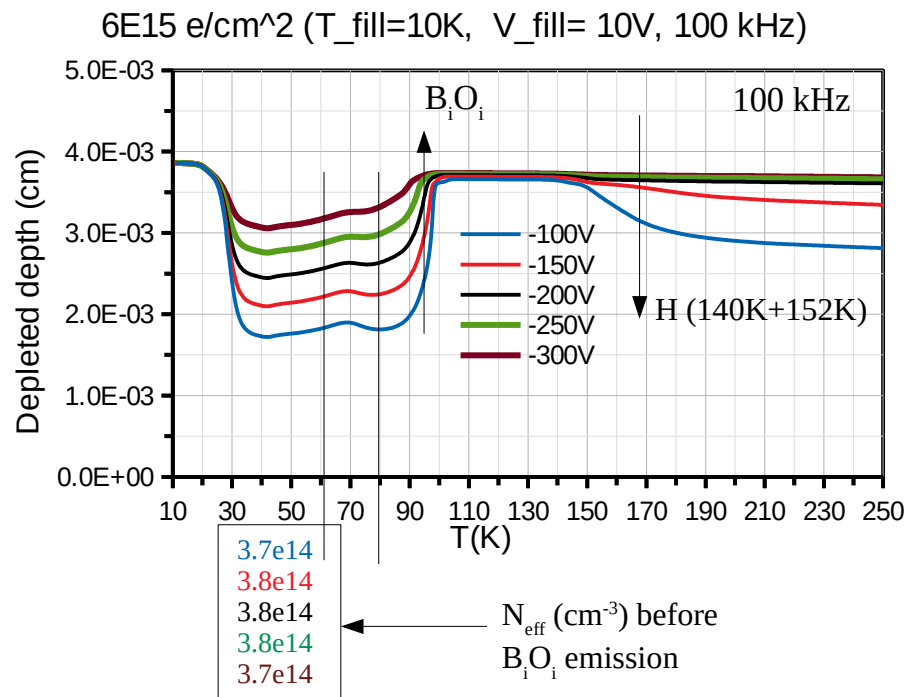
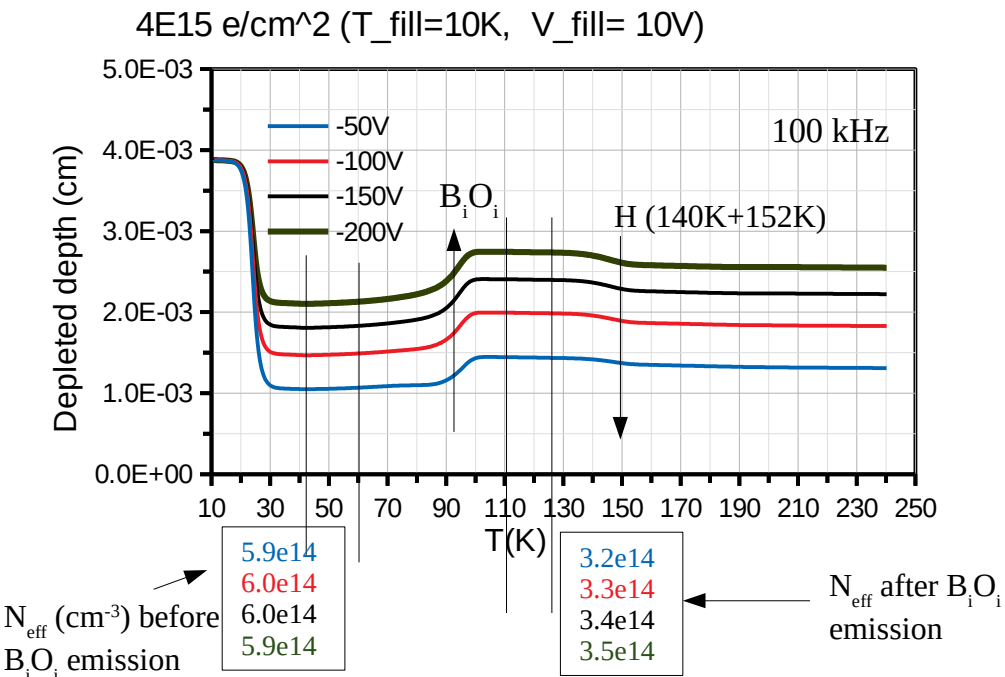
Annealing behavior of X-defect



TS-Cap measurement analysis



Example of TS-Cap on B_iO_i (10 Ωcm , as-irrad)



- Depleted depth was extracted from TS-cap with $d = \epsilon_{\text{si}} \epsilon_0 A / C$
- The shift of B_iO_i peak temperature versus V_{bias} can also be observed in TS-Cap measurement
- Freeze-out of free charge carriers for $T < 40\text{K}$
- Effective doping concentration can be extracted only if the diode is not fully depleted

Basic principle(1-D)

Poisson equation: $\frac{dE}{dx} = \frac{q_0 N_{eff}}{\epsilon \epsilon_0}$

Occupation fraction: $f(T) = \exp\left(-\frac{1}{\beta} \int e_n dT\right)$

Effective doping during emission:

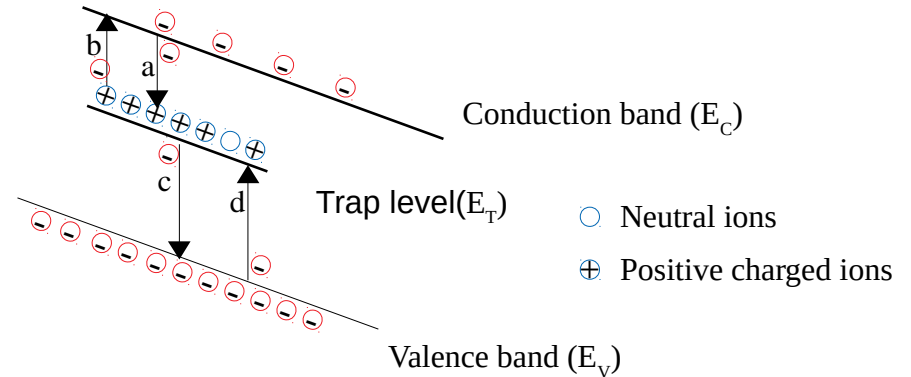
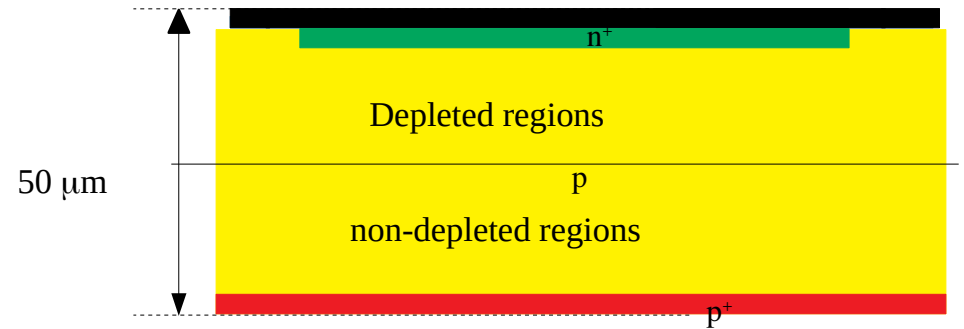
$$N_{eff} = N_0 + N_t \cdot (1 - f(T))$$

3-d Poole Frenkel ($\gamma = (qE/\pi\epsilon_0\epsilon_r)^{1/2}q/(k_B T)$):

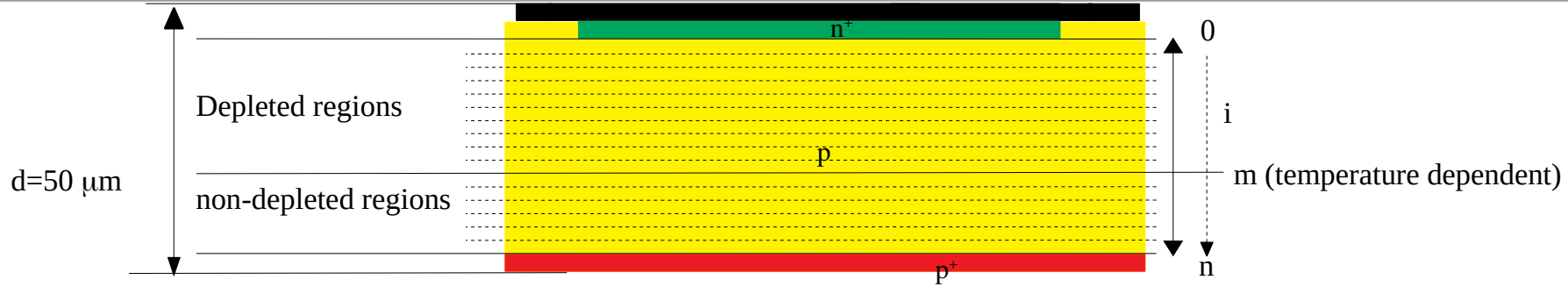
$$e_n = \sigma_n v_{th,n} N_c \times \exp\left(\frac{-Ea_0}{K_b T}\right) \left[\left(\frac{1}{\gamma^2}\right)(e^\gamma(\gamma-1)+1) + \frac{1}{2}\right]$$

Capacitance:

$$C = \frac{\epsilon \epsilon_0 A}{d}$$



Finite element (Basic principle)



Simplification (t for temperature T(K), i stands for position):

Poisson equation ($i < m_i$):

$$E_{i+1,t} - E_{i,t} = \frac{q_0 \text{Neff}_{i,t} \cdot d_t}{\epsilon \epsilon_0 \cdot n} \quad \text{and} \quad E_{i,t} = \sum_{j=0}^{m_i} \frac{q_0 \text{Neff}_{j,t} \cdot d}{\epsilon \epsilon_0 \cdot n} - \sum_{j=0}^i \frac{q_0 \text{Neff}_{j,t} \cdot d}{\epsilon \epsilon_0 \cdot n}$$

$$\sum_{i=0}^{m_i} E_{i,t} \cdot \frac{d}{n} = V$$

Occupation fraction:

$$f_{i,t} = \exp\left(-\sum_t e_{n,i,t}\right)$$

Effective doping during emission:

$$\text{Neff}_{i,t} = N_0 - N_t \cdot (1 - f_{i,t})$$

3-d Poole Frenkel ($\gamma_{i,t} = (qE_{i,t} / \pi \epsilon_0 \epsilon_r)^{1/2} q / (k_B t)$):

$$e_{n,i,t} = \sigma_n v_{th,n} N_c \times \exp\left(\frac{-E_{a0}}{k_B t}\right) \left[\left(\frac{1}{\gamma_{i,t}^2}\right) (e^{\gamma_{i,t}} (\gamma_{i,t} - 1) + 1) + \frac{1}{2} \right]$$